JMEPEG
https://doi.org/10.1007/s11665-021-05650-2

1059-9495/$19.00

Temperature Effect on Twin Initiation during Equal-Channel Angular Pressing and Mechanical Properties of Twinning-Induced Plasticity Steel

Yuntao Xi, Lei Wang, Xinfa Zhang, Jun Xu, Shubin Lei, Yueming Feng, Xinyue Hao, and Daoyong Yang

Submitted: 15 December 2020 / Revised: 27 January 2021 / Accepted: 31 January 2021

To examine the effect of temperature on twinning initiation and strain accumulation, a twinning-induced plasticity (TWIP) steel with chemical composition of Fe-25Mn-1.66Si-1.23Al was successfully prepared and subjected to severe plastic deformation (SPD) with equal-channel angular pressing (ECAP) at room temperature and warm temperature (300 °C), respectively. The microstructure was analyzed using different techniques, while its mechanical properties were measured by performing micro-tensile tests before and after the ECAP procedure. With such analyzed microstructure after ECAP procedure, the grains of the investigated TWIP steel are found to be elongated and the grain size decreases sharply especially at room temperature, compared to that before the ECAP procedure. The transmission electronic microscope (TEM) micrographs confirmed the existence of twins in all ECAP extruded conditions; however, at room temperature and after multiple passes of ECAP process at a higher temperature, it is easier to initiate secondary twins with a complex morphology. One pass of ECAP at room temperature can cause a strain effect of two passes at 300 °C. Strain hardening behavior was analyzed through $\ln(d\sigma/d\varepsilon) - \ln\sigma$ plot; the results show that the annealing samples present a relatively high strain hardening capability while the strain hardening capability of ECAP-ed samples reduces gradually with the amount of total strain applied by the ECAP.

Keywords ECAP, mechanical behavior, temperature, twins, TWIP steel

1. Introduction

Over the past decade, a new group of medium- and high-manganese (Mn) steel such as transformation-induced plasticity (TRIP) steels and twinning-induced plasticity (TWIP) steels with low stacking fault energy (SFE) has attracted great interests of researchers from materials science. Due to its high content of Mn, TWIP steel has an intermediate SFE range (i.e., 15-40 mJ/m^2) at room temperature, and thus, the twinning mechanism is one of the main characteristics of deformation (Ref 1). Such twinning mechanism is known as the dynamic Hall–Petch effect or TWIP effect, resulting in a hindered movement of dislocations and an improved strain hardening rate. It has been proved that TWIP steels with 20-30% Mn content have a great potential in the automotive industry owing to their excellent strength and ductility as a result of the formation of mechanical twins during deformation (Ref 2-4).

Although a defect of low yield strength seriously limits the extensive applications of TWIP steels (Ref 5), numerous efforts have been made to tackle such a technical challenge from various aspects such as pre-deformation (Ref 6, 7) and recovery annealing (Ref 8-10). In practice, grain refinement is considered to be the best way to improve the mechanical properties of the TWIP steel since SFE can be maintained and twinning is the favorable deformation mechanism (Ref 11-13). By, respectively, imposing high pressure torsion (HPT) on different TWIP steels, Matoso et al. (Ref 14) and Abramova et al. (Ref 12) significantly improved their hardness. By fabricating the gradient TWIP steels with surface mechanical grinding treatment (SMGT), Ding et al. (Ref 15) formed a multilayer structure containing twins. To process the TWIP steels through accumulative roll bonding (ARB) at room temperature, Etemad et al. (Ref 16) showed that, with an increasing strain, the primary and secondary mechanical twins as well as the hierarchical nanotwinned (HNT) structures were gradually formed in the TWIP steel. Also, Yu et al. (Ref 17) found that nanocrystalline and nanotwin appear in the TWIP steels during a cold-rolling process when rolling reduction is more than 90%.

Among numerous grain refinement methods, it is well recognized that equal-channel angular pressing (ECAP) procedure of severe plastic deformation (SPD) can be used to efficiently enhance the steel yield and its ultimate strength (Ref 18-22). Nevertheless, it is difficult to carry out the ECAP on TWIP steel

Yuntao Xi, School of Material Science and Engineering, Xi'an Shiyou University, Xi'an 710065, China; and Petroleum Systems Engineering, Faculty of Engineering and Applied Science, University of Regina, Regina, SK S4S 0A2, Canada; **Lei Wang**, School of Material Science and Engineering, Xi'an Shiyou University, Xi'an 710065, China; and State Key Laboratory of Metastable Materials Science and Technology, Yanshan University, Qinhuangdao 066004, China; **Xinfa Zhang** and **Jun Xu**, National Engineering Laboratory for Exploration and Development of Low-Permeability Oil and Gas Fields, Xi'an 710018, China; and CCDC Drilling and Production Technology Research Institute, Xi'an 710018, China; **Shubin Lei, Yueming Feng,** and **Xinyue Hao**, School of Material Science and Engineering, Xi'an Shiyou University, Xi'an 710065, China; **Daoyong Yang**, Petroleum Systems Engineering, Faculty of Engineering and Applied Science, University of Regina, Regina, SK S4S 0A2, Canada. Contact e-mails: ytxi@xsyu.edu.cn, wanglei@xsyu.edu.cn, richard0723@163.com, and tony.yang@uregina.ca.

Published online: 25 March 2021

due to its extremely high strength and high ductility. Previous attempts to process TWIP steel in ECAP dies with an inner angle of 90° at room temperature failed due mainly to fractures in the punch (Ref 23, 24). Bagherpour et al. (Ref 25) conducted an ECAP procedure for TWIP steels in an ECAP die with an inner angle of 120° at room temperature, resulting in a large number of cracks. Recently, the ECAP procedures on TWIP steel have been conducted at elevated temperatures (Ref 23, 24, 26). By conducting ECAP procedure on a FeMnC TWIP steel at different temperatures, Timokhina et al. (Ref 23) correlated the microstructure characteristics to the morphology of twins and dislocations. With four passes of ECAP on a FeMnCAl TWIP steel, Haase et al. (Ref 24) found that a microstructure of grain refinement results in the enhancement of the tensile strength with a limited ductility.

In the process of plastic deformation, a temperature difference affects the nucleation probability of twinning in TWIP together with its mechanical properties. Since the recovery and recrystallization caused by the temperature rise affect its formation, a twin system initiated by a lower plastic strain at room temperature may be equal to or even higher than that with a larger plastic strain at an elevated temperature. So far, limited attempts have been made to examine the effects of temperature and strain on twin initiation and mechanical properties of TWIP steel.

In this study, an integrated framework has been developed to not only examine temperature effect on twin initiation during ECAP, but also determine the corresponding mechanical properties of TWIP steels. More specifically, the ECAP process of TWIP steel at different temperatures will be conducted, and the microstructure will be detected through electron backscattered diffraction (EBSD) and transmission electronic microscope (TEM), while its mechanical properties will be measured by performing micro-tensile tests in this work. The effects of temperature and strain on twin initiation, morphology, and mechanical properties will be investigated. Through this work, the microstructure of TWIP steel at different temperatures and its influence on mechanical properties can be better understood.

2. Experimental

2.1 Materials

The chemical composition of the TWIP steel used in this study is tabulated in Table 1 in which the calculated SFE based on references (Ref 27, 28) is also included. In this work, the calculated SFE value would allow twinning as the favored deformation mechanism (Ref 29).

2.2 Experimental Procedures

2.2.1 ECAP Tests. Firstly, the TWIP steel was cast into ingots, and air cooling was adopted. After casting, forging procedure was carried out to close possible pores and homogenize the chemical composition and microstructure. Then, cylindrical samples of 8 mm in diameter and 60 mm in length were cut from the forged ingot for the ECAP tests. All bars were annealed at 1200 °C for 1 h in a protective Ar inert atmosphere in order to eliminate inhomogeneous microstructure and segregation which were formed during solidification, followed by water quenching to room temperature.

Table 1 The chemical composition of the investigated TWIP steel in weight percentage and the SFE value

C	Mn	Si	Al	Fe	SFE, mJ/m^2
0.27	25	1.66	1.23	Bal.	24.5

The ECAP procedure was performed in a solid die made by a tool steel insert with two channels intersecting at an inner angle of $\Phi = 90°$ and an outer angle of $\psi = 37°$ (see Fig. 1). According to the calculated strain with the correlation given by Iwahashi et al. (Ref 30), each pass can result in true stain more than 100%. The extrusion speed was 0.002 m/s (i.e., the corresponding strain rate was 3.3×10^{-2} s^{-1}), and MoS2 was used as a lubricant. The ECAP route adopted was BC (i.e., the sample is rotated 90° between compression passes, while the rotation is always kept in the same direction). To compare the counteracting effect of temperature on the true strain and the effect of strain on twin initiation, the ECAP procedure was conducted at different temperatures. At room temperature, the investigated TWIP steel was extruded for one pass of ECAP procedure, while four isothermal passes were further performed at 300 °C. This temperature is selected because 300 °C is the lowest temperature for multi-passes ECAP in the current research. At the elevated temperature of 300 °C, the die was placed inside a furnace for warm processing, and then, the sample was introduced in the die and kept for five minutes before processing.

2.2.2 EBSD Tests. With a field emission gun JEOL JSM-7001F (FE-SEM) operated at 20 kV, the EBSD analyses were carried out to characterize the microstructure. The EBSD samples were cut from the center of the ECAP-ed samples and then ground and polished using diamond paste, and a final stage was polished by a vibration polishing machine (VibroMet 2) with 0.02 μm colloidal silica solution. The scanning procedure was performed on the transverse plane of the sample processed by the ECAP (*xy* plane, see Fig. 2). The axis reference system *xyz* is also illustrated in Fig. 2, indicating the extrusion direction "*x*" (ED), the normal direction "*y*" (ND) and the transverse direction "*z*" (TD). Different scan step sizes were used: 3.00 μm for the TWIP steels under the annealed condition, 0.20 μm for the samples with 1 ECAP pass, 0.05 μm for the samples with 2 ECAP passes, and 0.03 μm for the samples with 4 passes. The indexation rate was maintained almost at 70% for the samples after the ECAP procedure. They were post-processed utilizing the HKL Channel 5 software. The grain boundaries were identified as high-angle grain boundaries (HAGB) in which misorientation was above 15°, while sub-grain boundaries were low-angle grain boundaries (LAGB) with a misorientation between 2° and 15°. For the twin boundaries, a specific misorientation of 60° over the $<111>$ axis was taken.

2.2.3 TEM Tests. Further microstructure examination was performed through TEM. The specimens were analyzed in a Philips C2100 microscope operating at 200 kV. The samples for TEM observation were mechanically polished to 40 μm in thickness and then thinned by twin-jet electron polishing in an electrolyte solution of 95 vol.% acetic acid glacial and 5% perchloric acid at room temperature.

2.2.4 Tensile Tests. In the central region of the ECAP sample, grains underwent severe deformation, showing more grain refinement, i.e., near the edge of the sample, there is relatively less grain refinement. Therefore, the samples used for

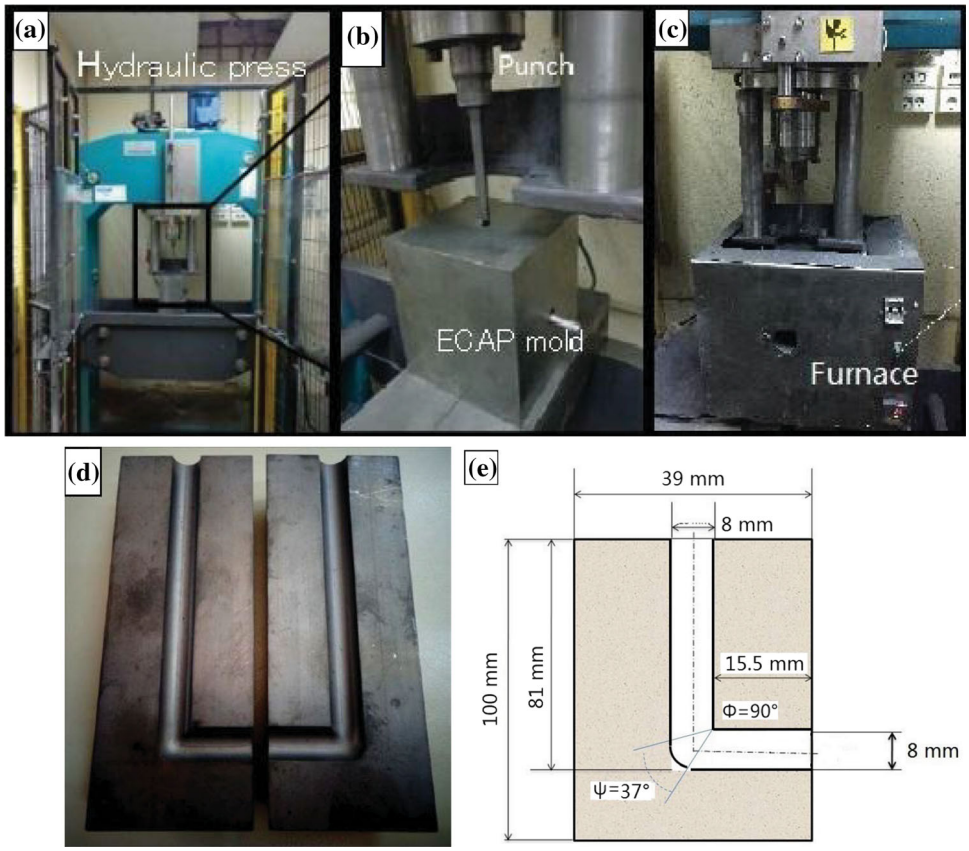

Fig. 1 ECAP system and mold and insert dimensions: (a) hydraulic press, (b) ECAP mold, (c) furnace, (d) actual drawing of ECAP mold, and (e) die dimension drawing of ECAP mold

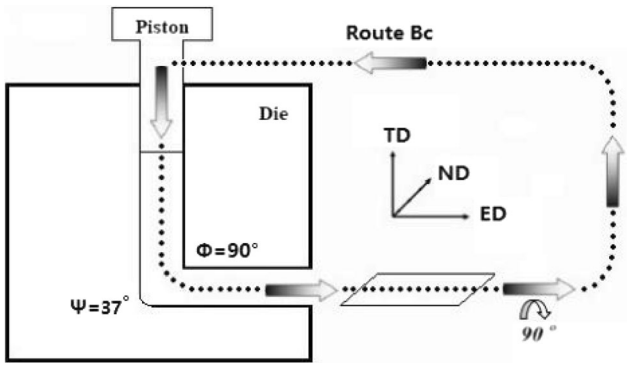

Fig. 2 ECAP die configuration and the corresponding coordinates system used in the current research: ND (normal direction), ED (extrusion direction), and TD (transverse direction)

the tensile tests should avoid effects due to material heterogeneity. For this reason, the tensile testing specimens were machined from the middle of the rod cross-sectional sample. On the other hand, owing to the reduced dimension of ECAP-ed material, a standard tensile sample could not be machined from the bars. Hence, the micro-tensile sample was cut with gauge length of 3 mm. (A detailed dimension is given in Fig. 3.) The tensile testing was carried out in an micro-test DEBEN machine with a cross-head speed of 3.3×10^{-3} mm/s (quasi-static loading conditions) in the longitudinal direction at room temperature. Each group of tensile tests was repeated with three samples.

3. Results

3.1 Microstructure Characterization

3.1.1 Annealing Treatment. Figure 4 shows the optical microscope images and more detailed EBSD information of the investigated TWIP steel after the homogenization heat treatment. As can be seen in Figure 4(a) and (b), the microstructure in terms of grain size is homogeneous. In particular, the average grain size is measured to be 123.5 and 199.6 μm with and without considering twin boundaries, respectively. By performing EBSD analyses, grain boundaries, sub-grain boundaries and twin boundaries can then be identified according to the misorientation. A color code has also been assigned to identify the different boundaries with the EBSD tests: Grain boundaries correspond to the black lines, green lines are sub-grains, and twins appear as white lines.

The feature of the boundaries in the TWIP steel after homogenization heat treatment can be observed in Fig. 4(c). In this case, almost no sub-grains are noticed, and special grain boundaries of twin type are obvious. These twin boundaries are directly resulted from the heat treatment and can be considered as annealing twins, which are easily identified because they appear as straight lines in the microstructure and often appear in pairs of parallel lines due to their characteristics stacking sequence (Ref 26). Figure 4(d) shows the grain diameter

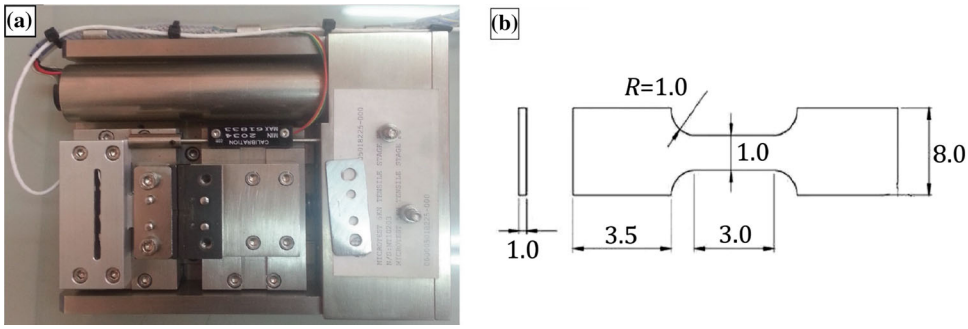

Fig. 3 (a) Micro-tensile test machine and (b) dimensions of micro-tensile samples (in mm)

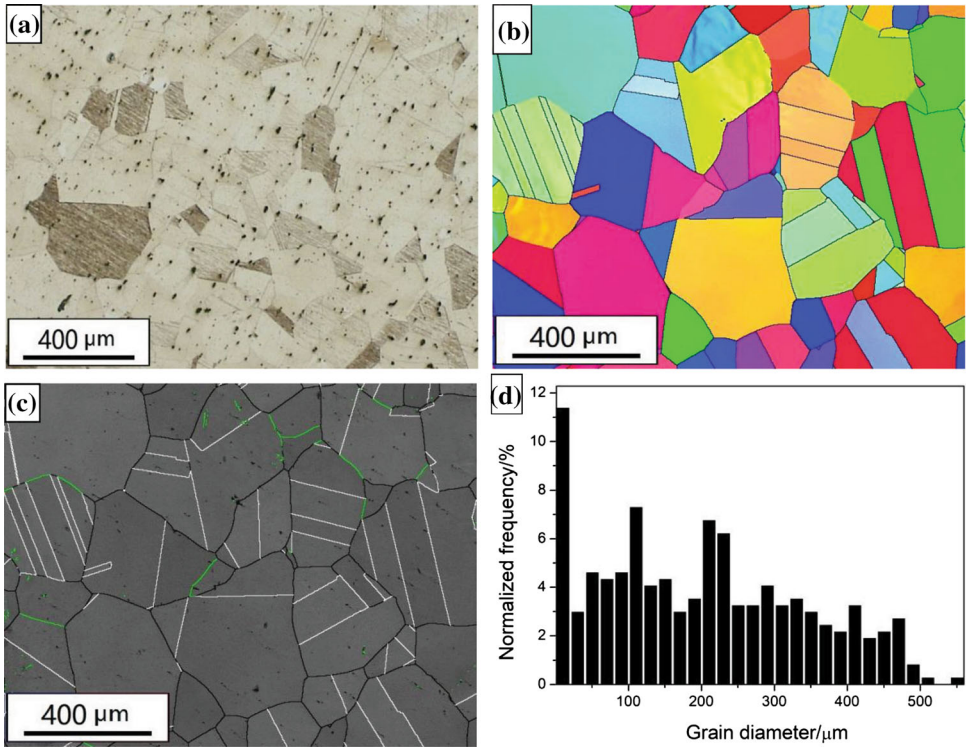

Fig. 4 (a) Optical microscope image and EBSD analysis of the investigated TWIP steel in annealing condition: (b) inverse pole figure (IPF) grain map; (c) grain boundary map (black line—high-angle grain boundary, green line—low-angle grain boundary, white line—twin boundary), and (d) grain size distribution (Color figure online)

distribution for the TWIP steel with the annealing treatment. It can be noticed that the grains consist of different sizes, but most of them are similar in size.

3.1.2 Microstructure of the TWIP Steel ECAP-ed. *3.1.2.1 Room Temperature.* After one ECAP pass at room temperature, the grains appear extremely elongated in the shear direction, whereas the average grain size is sharply reduced. Specifically, the grain size reduces sharply from 199.6 μm to less than 3.00 μm, and a large amount of LAGB is generated during one pass as illustrated in Fig. 5(a) and (b). In addition, the microstructure of the investigated TWIP steel is highly heterogeneous, with the presence of mechanical twins in some regions and very fine grains occur in other regions of the sample (see Fig. 5a). In fact, all mechanical twins with the same grain align with the same orientation. (This is also evident in the grain boundary map in Fig. 5b.) The orientation of the twins is related to the initial orientation of the grains, and the fact that all twins align with the same orientation indicates that all of them have formed inside the same original grain. After one pass at room temperature, the fraction of new fine grains is found to be higher than that for the sample ECAP-ed at 300 °C (as detailed in the next section). From Fig. 5(a), it can be seen that fine grains are located in regions with high fractions of LAGB, indicating that fine grains appear by the transformation of previous sub-grains.

As illustrated in the EBSD analyses, significant changes in the microstructure are observed after one ECAP pass at room temperature, i.e., many austenite grains contain a large number of deformation twins. This phenomenon is more obvious from the TEM analysis, as indicated in Fig. 5(c), (d) and (e). In the general view of TEM observation in Fig. 5(c), a large number of deformed twins with a thickness of about 50-200 nm can be seen. The thickness of twins in TEM is similar to that observed

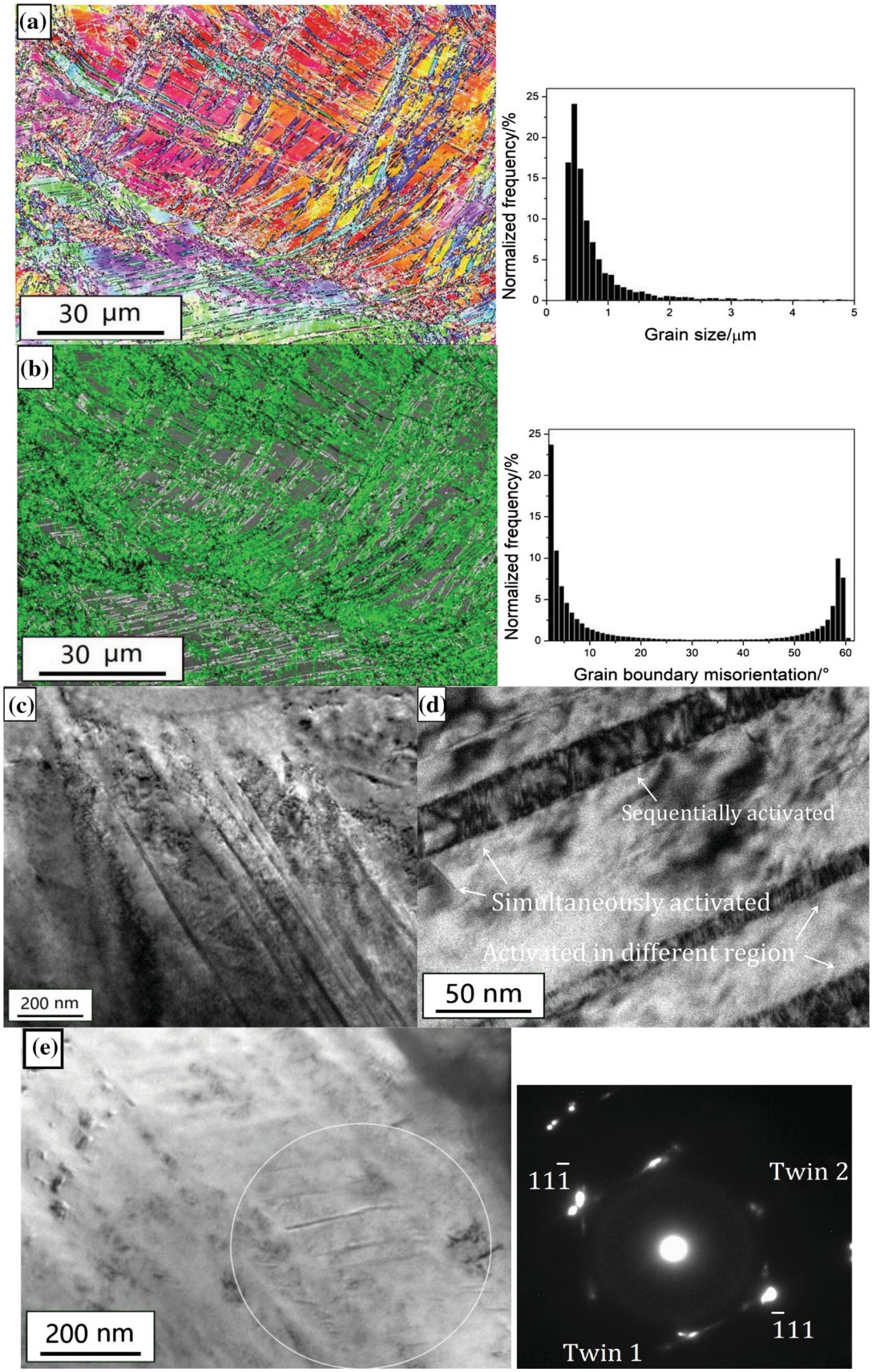

Fig. 5 Microstructure of the investigated TWIP steel ECAP-ed one pass at room temperature: (a) EBSD general grain map, (b) EBSD grain boundary map, (c) TEM general view of twins, (d) different types of secondary twin system, and (e) SAED of two twin system

by the EBSD analyses. Furthermore, such primary twins are located in some regions of the sample forming bundles. Interestingly, after ECAP at room temperature, numerous types of secondary twinning are activated, as shown in Fig. 5(d) and (e). Babier et al. (Ref 31) described three different types of secondary twin system: (i) two systems sequentially activated; (ii) two twinning systems simultaneously activated; and (iii) two systems activated in different regions. Therefore, all three types of secondary twins can be identified in the sample ECAP-ed at room temperature, as shown in Fig. 5(d). Such observed SAED pattern confirms the existence of two different twin systems by relating the extra diffraction spots of two different perpendicular twin systems formed on the $(11\bar{1})$ and $(\bar{1}11)$ planes, as depicted in Fig. 5(e). The twin system network can be obtained by a 180° rotation of the matrix reciprocal lattice around the $[11\bar{1}]^*$ reciprocal direction. This finding is consistent with those documented elsewhere (Ref 31).

3.1.2.2 Elevated Temperature. The four isothermal passes were performed at 300 °C for the current TWIP steel, and the typical micrographs of EBSD and TEM characterization are illustrated in Fig. 6, 7 and 8, respectively. As for the first-pass sample shown in Fig. 6(a), it is observed from the EBSD-IPF grain map that there are large elongated grains together with very fine equiaxed grains, which is surrounded with the former. As can be found in Fig. 6(b), twinning is acted as a deformation mechanism and indicated with white lines. After one pass of the ECAP process at 300 °C, there is a considerable amount of twin boundaries; however, the fraction of twin boundaries after the ECAP procedure at an elevated temperature of 300 °C is much lower than that at room temperature. On the other hand, there are a few fine grains formed during one pass of the ECAP procedure, as shown in Fig. 6(a). Even though the proportion of fine grains is not high, the grain size of such newly formed grains is less than 5 microns. These fine grains are usually formed between two large elongated neighboring grains. (Grain boundaries are represented as black lines.) Another feature in one-pass sample is the formation of numerous LAGB in some large elongated grains, as indicated with green lines in Fig. 6(b).

Figure 6(c), (d), and (e) shows the TEM information of the one-pass TWIP steel deformed at 300 °C, while Fig. 6(c) presents the general view of twins in the one-pass samples. The twin thickness at this stage is ranged between 200 and 400 nm. With performing a careful observation, a high dislocation density is observed inside the twins (Fig. 6d), which can be related to the large kinematic hardening. This finding is consistent with that found elsewhere (Ref 23). Grains with a more refined twin structure are also found, although less often than the grains with coarse twins are exposed in Fig. 6(c). In these cases, secondary twinning was frequently observed (Fig. 6e) as those described elsewhere in the TWIP steels deformed by ECAP at 300 °C (Ref 23).

After two ECAP passes, the microstructure still shows some heterogeneity as shown in Fig. 7(a), though the overall fraction of equiaxed grains formed around the large grains seems to increase. The twin boundaries as depicted by the white lines in grain boundary map (see Fig. 7b) can be detected as well, while the size of the fine grains has been reduced to 1-2 microns. Moreover, it can be seen that some of the newly formed grains are inside the large grains, indicating that these fine grains are transformed from sub-grains and the large grain is under a refinement process. The formation of sub-grains reveals that there are still numerous LAGBs in large grains.

The TEM images corresponding to the samples after two ECAP passes are presented in Fig. 7(c) and (d). Compared with the first ECAP pass, a more comprehensive grain refinement is formed during the second ECAP pass after which a certain degree of twin boundaries are formed. In TEM micrographs as illustrated in Fig. 7(c), it is comparatively easy to observe grains in which bundles of twins are formed. The thickness of such formed twins is measured about 50-100 nm, which is significantly reduced, compared with that of one pass. This finding agrees well with the statement that the twin thickness declines as the grain size decreases (Ref 5). Inside these primary twins, the dislocation density is very high as that in the case of one-pass ECAP sample, and the dislocations gradually form cellular structure. Similar to one-pass TWIP steel, formation of a secondary twinning system inside primary twins is detected in the second-pass sample. After the second ECAP pass, the secondary twin system appears more frequently with more complex morphology.

After four ECAP passes at 300 °C shown in Fig. 8(a), the heterogeneous microstructure remains, although less elongated grains can be observed and the presence of new fine grains is more extensive. As illustrated by white lines in Fig. 8(b), twinning is still an important deformation mechanism of the TWIP steels after four ECAP passes. In some parts of microstructure as shown in Fig. 8(a), the fine grains start to show an equiaxed morphology with grain size less than 1 micron. Figure 8(b) reveals that some of the sub-grains are transforming into new fine grains. This means that increasing the number of ECAP passes could promote a larger amount of HAGBs, and thus, larger strength could be expected.

The microstructure of the four ECAP passes for the TWIP steel has been refined again comparing with two ECAP pass samples; however, dislocation density and grain size change with a low rate. This phenomenon may imply that the capability of TWIP steel to increase the density of defects is small. Similarly, numerous different twin systems are activated in the four ECAP passes as shown in Fig. 8(c). After multi-pass of ECAP, the thickness of some twins decreases significantly within a range of 30-40 nm as depicted in Fig. 8(d).

3.2 Mechanical Behavior

Figure 9(a) shows the true stress–strain curves of the investigated TWIP steel with different numbers of ECAP passes at 300 °C and one ECAP pass at room temperature, respectively. As can be seen, there exists a significant increase of both yield strength (YS) and ultimate tensile strength (UTS) induced by the ECAP procedure. Especially for one-pass sample, the corresponding YS sharply increases near 5 times (from 188 to 1018 MPa) at an elevated temperature and increases more than 7 times (to 1400 MPa) at room temperature. The maximum YS and UTS are obtained in four passes for the TWIP steels, and the corresponding values are 1530 and 1603 MPa, respectively. After the ECAP procedure, the ductility decreases gradually; however, the 8.5% elongation of four passes from the ECAP-ed samples at 300 °C and 13% elongation of one ECAP-ed pass at room temperature are still appealing. This type of behavior can be attributed to the strain hardening related to the interaction between dislocations and twins (Ref 32).

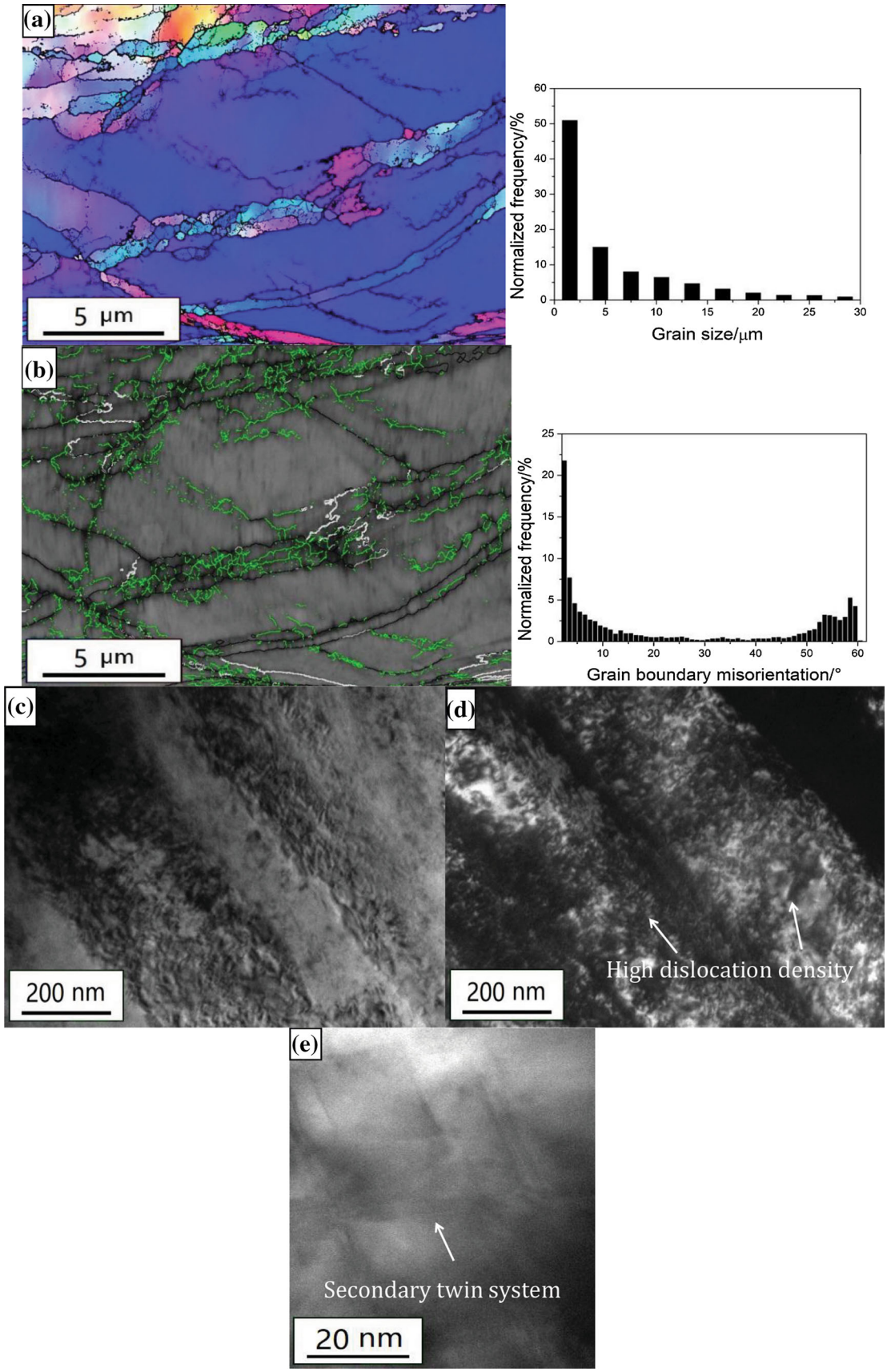

Fig. 6 Microstructure of the investigated TWIP steel ECAP-ed one pass at 300 °C: (a) general grain map, (b) grain boundary map, (c) TEM general view of twins, (d) high dislocation density inside the twins, and (e) secondary twin system

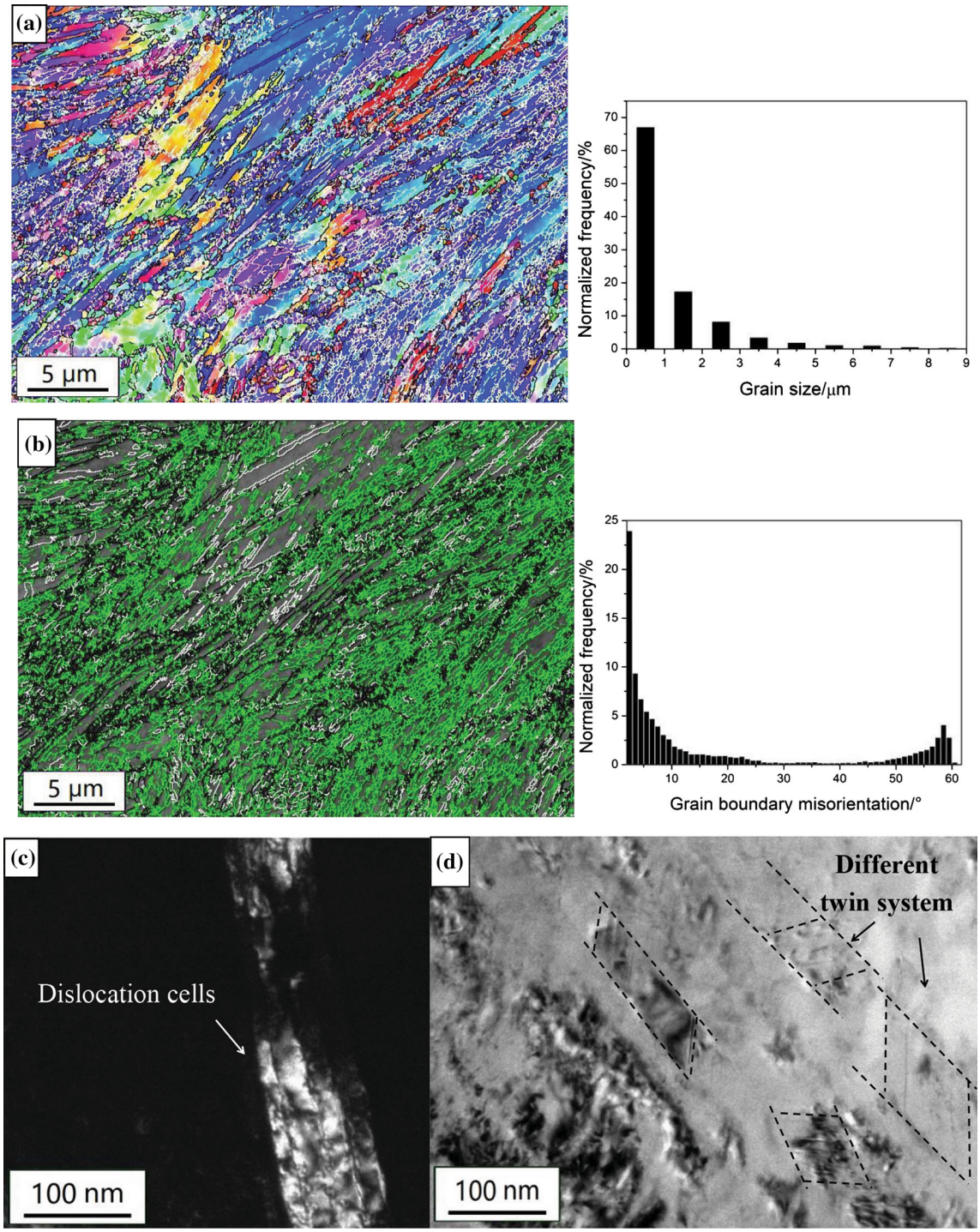

Fig. 7 Microstructure of the investigated TWIP steel ECAP-ed two pass at 300 °C: (a) general grain map, (b) grain boundary map, (c) TEM general view of twins and dislocation cells, and (d) different twin system

Figure 9(b) illustrates the strain hardening rate versus true strain for the TWIP steel under different deformation conditions. In a similar way to what was found for other TWIP steels (Ref 26), the annealing samples show a relatively high strain hardening capability.

After a pronounced decrease up to strain of 0.05, the strain hardening capability starts to rise up and reaches a constant level in the intermediate strain, and then, it shows a slight decrease and reaches the second platform after strain of 0.25. Finally, over 0.32 true strain, the strain hardening rate decreases again until the specimen rupture is achieved.

On the other hand, the strain hardening capability of ECAP-ed samples reduces gradually with the amount of total strain applied by the ECAP. At an elevated temperature, the one-pass sample shows a reducing trend of strain hardening with the strain and reaches a nearly constant value at strain of 0.06, and the stain hardening rate reaches zero at 0.13 true strain. As for the second-pass sample, the constant period is only maintained

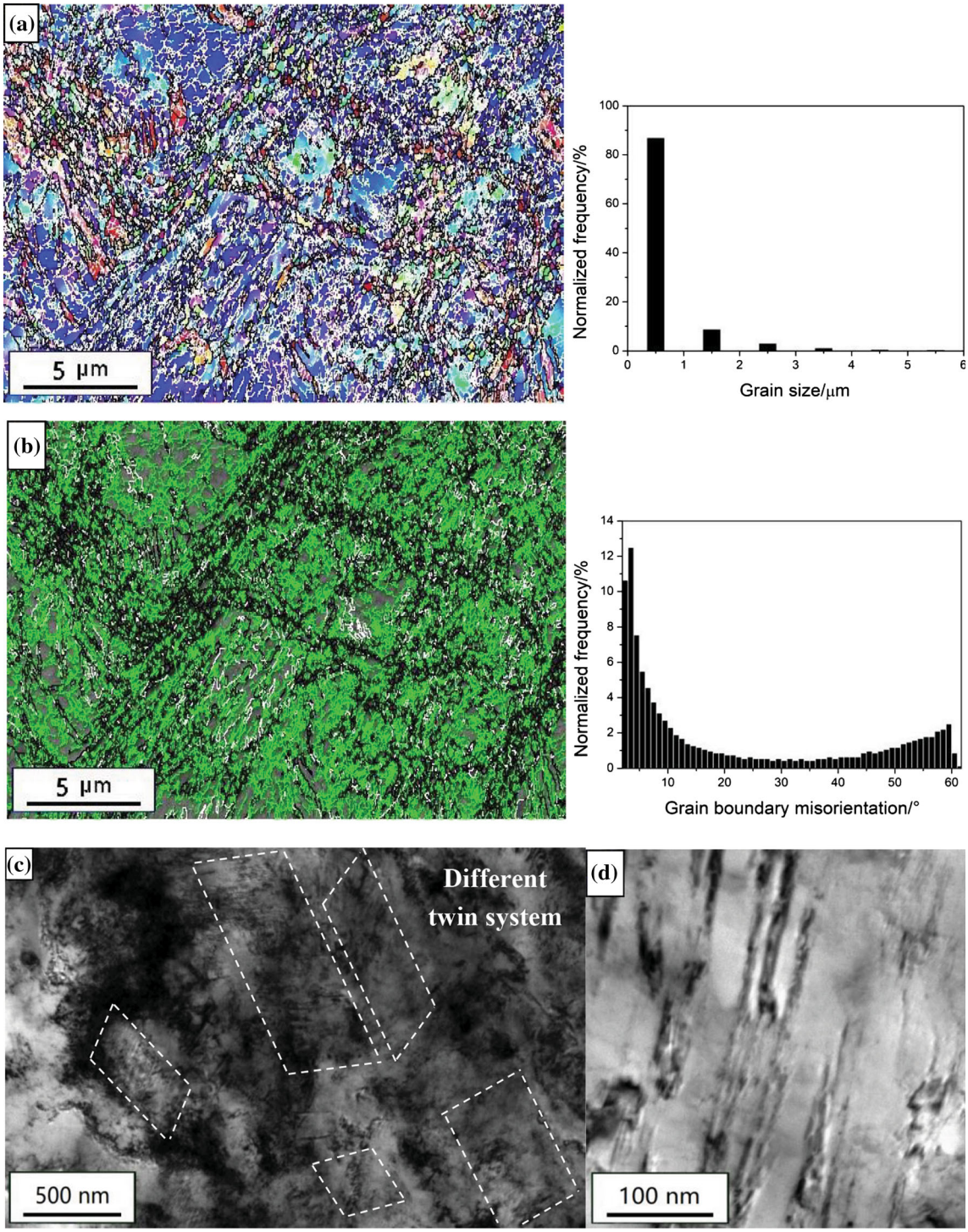

Fig. 8 Microstructure of the investigated TWIP steel ECAP-ed four passes at 300 °C: (a) general grain map, (b) grain boundary map, (c) TEM general view of twins system, and (d) magnification of twins

in a small strain range of 0.03-0.06 and then reaches zero at a strain of 0.08. As for the samples with four passes, there is almost always softening in the plastic region and the strain hardening quickly reaches zero after a strain of 0.02. For the ECAP-ed sample at room temperature, it shows a comparatively low strain hardening capability only at a small region of strain, and then, it reaches an extremely short plateau and then falls to zero.

4. Discussion

4.1 Twin Formation

The formation of twins in the ECAP-ed samples can be attributed to two factors: (i) formation mechanism of SFE and (ii) effect of SPD. In this work, the SFE value of the investigated TWIP steels is in the range of values where

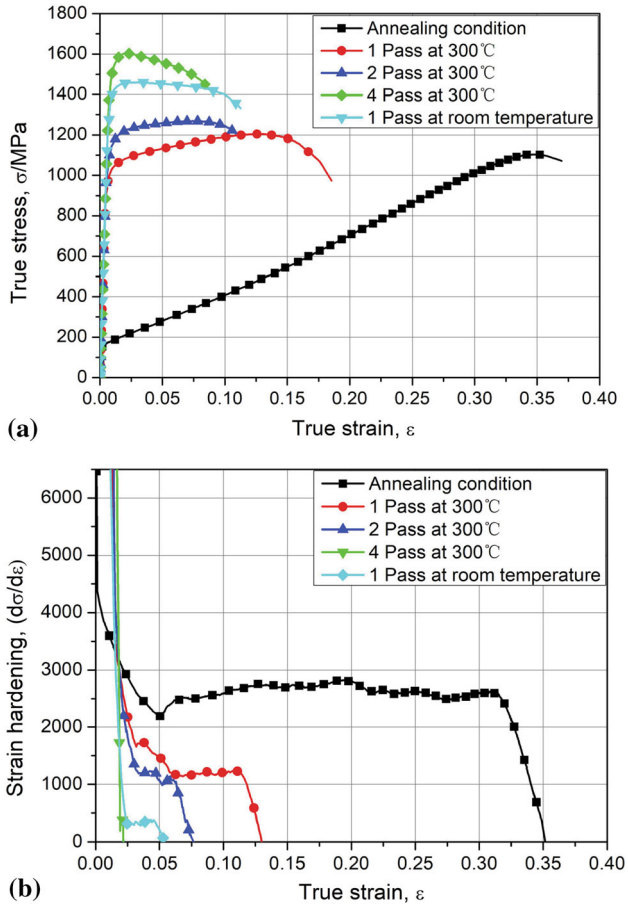

Fig. 9 (a) Tensile true stress–strain curves of the TWIP steels in different conditions and (b) strain hardening rate vs. true strain for samples

twinning is an active deformation mechanism and stacking fault is the source of deformation twins (Ref 4, 5).

With an increased temperature, the amount of mechanical twins and the fraction of twined grains are reduced. As being universally accepted, the increase of temperature will seriously affect the value of SFE and thus the probability of twin formation. According to previous studies (Ref 33, 34), when the temperature is increased (above 300 °C), the SFE of steels can reach 60 mJ/m^2, leading to deformation twinning to be deactivated (Ref 35). Numerous efforts have found that when the tension deformation temperature is higher than 300 °C, no twins can be observed during the tensile deformation of the TWIP steels (Ref 36, 37). Nevertheless, the true strain induced by a tensile process can only reach up to 0.4-0.5, which is much lower than that of an ECAP process. Zhu et al. (Ref 38, 39) indicated that deformation twinning is found to be a major mechanism during the SPD process even when grain size is extremely small. Shterner et al. (Ref 36) pointed out that the critical strain for mechanical twinning in the TWIP steels can be increased with an increase of deformation temperature, and thus, a high strain induced by the ECAP process provides necessary conditions for the formation of mechanical twins. Under a SPD process, the SFE is not the only property controlling the formation of twins, and twins can be observed even when the deformation is applied at high temperatures.

With regard to the influence of temperature, it is obvious that twin fraction and twin-ed grains of the ECAP-ed TWIP steels at room temperature are higher than that of the ECAP-ed samples at 300 °C with a downward trend of twin thickness. More specifically, at room temperature, the thickness of mechanical twins produced by the ECAP is about 50-200 nm, which is similar to the twin thickness after two passes at 300 °C. To a certain extent, it reflects that one pass of ECAP at room temperature can cause strain effect of two passes at 300 °C. Additionally, deforming at room temperature activates more secondary twinning systems. As mentioned earlier, all secondary twinning systems, as described in the literature, can be found for the sample ECAP-ed at room temperature, whereas only the sequentially activated twinning system was detected for the sample pressed one pass at 300 °C (see Fig. 6e). This can be explained in terms of the strain accumulation achieved at the different deformation temperatures. At 300 °C, the accumulated strain is lower because there is possibility for a certain degree of dynamic recovery with less probability as well as dynamic recrystallization. The higher the accumulated strain, the easier the activation of secondary twining systems, as reported by Barbier et al. (Ref 31).

Venables further proposed a model for the critical shear stress of twin nucleation (Ref 40) where L_{pile} is the characteristic length of dislocation stacking and υ is Poisson's ratio. It can be seen from the model that an increase of dislocation stacking characteristic length will lead to a decrease of the critical shear stress of twin nucleation, that is, twins are easier to form. At room temperature, dislocation stacking caused by severe strain is more obvious due to a limited effect of recovery, which is conducive to the formation of primary and secondary twin system (Ref 23, 24). At a high temperature, only after several ECAP passes, the corresponding strain can be accumulated to initiate the twin system. In fact, even at 300 °C, different secondary twinning systems can be activated when the number of ECAP passes is increased, as shown in Fig. 7(d) and 8(c). Based on the SFE values, however, the formation of twins is more difficult so that both primary and secondary twinning mechanisms are more rarely found in the sample ECAP-ed at 300 °C (Ref 41, 42).

4.2 Mechanical Behavior

The $\ln(d\sigma/d\varepsilon) - \ln\sigma$ plot of the annealed sample of the current TWIP steel is plotted in Fig. 10(a). As can be seen, the plastic deformation can be divided into five stages. After stage A (strain of 0-0.05), the strain hardening rate shows a upward trend in a longer strain range of 0.05-0.18, which is stage B. Then, a slight decrease period is denoted as stage C in a strain range of 0.18-0.24. In a strain range of 0.24-0.32, a slight increase is found and this is termed as stage D. Finally, the strain hardening rate drops. According to the previous work (Ref 26, 43), these stages can be ascribed to the following mechanisms: (1) The transition point from stage A to stage B corresponds to the onset of twinning within grains deformed by multi-slip; (2) the increase period of stage B can be due to the primary deformation twins; (3) stage C and stage D are attributed to the secondary deformation twins (downward trend is resulted from a lower twinning rate); and (4) stage E finally is initiated when the slowdown of twinning activity and the plastic instability occurs.

The $\ln(d\sigma/d\varepsilon) - \ln\sigma$ plot of the TWIP steel after different ECAP passes at 300 °C is illustrated in Fig. 10(b). Compared

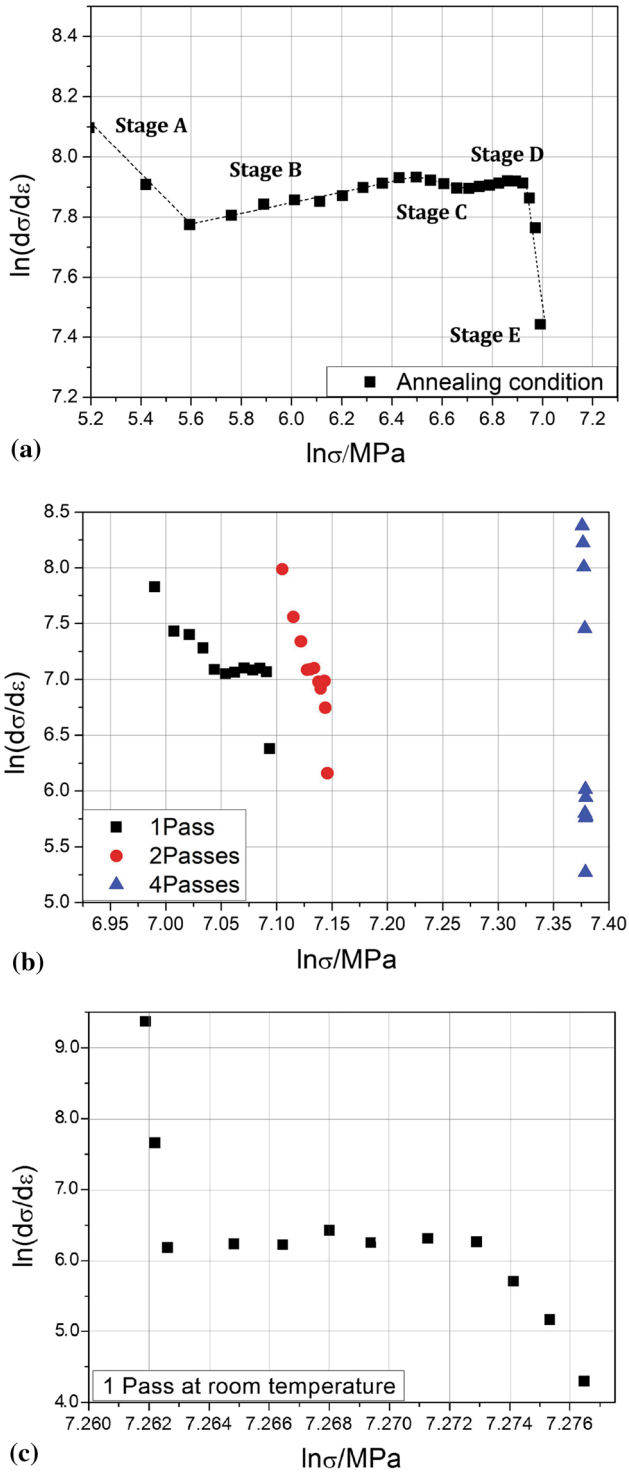

Fig. 10 The plot of ln(dσ/dε) vs. lnσ of the TWIP steel in (a) annealing condition, (b) after different ECAP passes, and (c) ECAP at room temperature

with the annealing condition sample, the strain hardening behavior (as given in Fig. 9b) and the ln(dσ/dε) − lnσ plots of the ECAP-ed samples show different characteristics. The plots for samples with two passes and four passes appear in the right-hand side because of a higher strength. Physically, the strain hardening behavior of all samples after the ECAP procedure shows that, after a downward trend, a slight increase in a small range of strain can be noticed and then it drops. The stage division is not similar to the corresponding annealing sample because the twinning capability is exhausted in a certain degree after ECAP process. In the subsequent tensile process, twin initiation ability is relatively limited, and the only transient rise can be attributed to twinning behavior. As for the sample with four passes of the TWIP steels, the strain hardening seems dropped extremely, indicating a lower twinning capability in these samples.

Regarding the strain hardening of the ECAP-ed sample with one pass at 300 °C, the material hardens up to a true strain of 0.13. From the analysis of microstructure by performing EBSD analyses in Fig. 5, it is clear that, although there is a certain degree of elongated grains with sub-grains or mechanical twins, other grains show less defects. Therefore, the material during the tensile tests at room temperature is still available to deform by mechanical twinning and dislocation slip. This analysis agrees with the one documented in Ref 44 for a TWIP steel with aluminum. In the case of two ECAP passes at 300 °C, the same trend is observed. The strain hardening behavior can be related to the evolution of the microstructure by the EBSD tests in Fig. 7(a). As can be seen, there is a significant reduction of grain size together with an increase of the number of fine sub-grains as a result of a high dislocation activity. Twinning activity was also observed in the TEM analysis in Fig. 7(c) and (d), where a large presence of nanotwins inside the primary twins is due to the occurrence of secondary twinning. Such detected twins are related to the inflection in the ln(dσ/dε) − lnσ plots. Finally, in the evolution of the strain hardening rate during tensile tests of the samples with four ECAP passes, the EBSD and TEM analyses showed that a large refinement of the microstructure has been achieved. Many sub-grains formed in the previous ECAP passes led to new fine grains with equiaxed morphology, while the remaining dislocation cells have reduced the diameter up to 100 nm or less and the mechanical twins appear being distorted with twin thicknesses around 30-40 nm. In addition, the evolution of dislocation density shows that the dislocation density is increased at a very low rate during the last two passes. All these observations led to the conclusion that, after 4 ECAP passes, the present TWIP steel reaches its saturation level and a small number of defects can be introduced during the tensile tests. As such, the strength for the four ECAP passes samples is the highest one, whereas the elongation is the shortest one. In this case, the strain hardening rate decreases continuously during the tensile test.

The ln(dσ/dε) versus lnσ plots of the TWIP steels ECAP-ed at room temperature for one pass are shown in Fig. 10(c). As can be observed, the temperature of ECAP procedure significantly affects the strain hardening behavior. The sample after an ECAP process at room temperature illustrates a lower capability of strain hardening than that ECAP-ed at 300 °C since the curve falls to a lower value (as shown in Fig. 9b). Through the EBSD and TEM analyses as shown in Fig. 5(b) and 6(b), a smaller number of deformed grains without defects are formed. When the tensile test is performed, the capability of deformation by mechanical twinning and dislocation slip for an ECAP-ed sample at room temperature is lower, and thus, the corresponding strain hardening capability is smaller.

5. Conclusions

A Fe-25Mn-1.66Si-1.23Al-0.27C TWIP steel was processed by the ECAP for one pass at room temperature and four passes at 300 °C, respectively. By performing the EBSD and TEM analyses, the evolved microstructure was detected, while the temperature effect was examined and analyzed. On the other hand, the relationship between microstructure and its tensile behavior was studied. The main conclusions are summarized as follows:

(1) Mechanical twins will exist after the ECAP process with different passes and different temperatures. When ECAP-ed at elevated temperatures, the formation mechanism of these twin boundaries is mainly due to effect of severe plastic deformation, while at room temperature, is primarily due to the effect of SFE. In addition, both strain and temperature dominate the twin initiation and twin thickness. One pass of ECAP at room temperature can cause a strain effect of two passes at 300 °C.
(2) The yield strength of TWIP steel sharply increases near 5 times after one ECAP pass at an elevated temperature and increases more than 7 times at room temperature for one-pass sample, while the elongation is still appealing. The annealing samples show a relatively high strain hardening capability, and the strain hardening capability of ECAP-ed samples reduces gradually with the amount of total strain applied, which is related to whether enough twins can be initiated.

Acknowledgments

The present work has been financially supported by Young scientific research and innovation team of Xi'an Shiyou University (Grant No. 2019QNKYCXTD14), State Key Laboratory of Metastable Materials Science and Technology (Grant No. 202111) and the China Petroleum Science and Technology Innovation Fund (Grant No. 2018D-5007-0216). The authors also acknowledge a discovery Grant and a Collaborative Research and Development (CRD) Grant from the Natural Sciences and Engineering Research Council (NSERC) of Canada to D. Yang.

Conflict of interest

The authors declare no conflict of interest.

References

1. L. Wang, J.A. Benito, J. Calvo and J.M. Cabrera, Twin-Induced Plasticity of an ECAP-Processed TWIP Steel, *J. Mater. Eng. Perform.*, 2017, **26**(2), p 554–562
2. J. Chen, J.J. Wang, G. Yuan and C.M. Liu, Twin Boundary Bending During Tensile Deformation and Its Temperature Dependence, *Mater. Sci. Eng. A*, 2019, **759**, p 47–54
3. R. Mohammadzadeh, Deformation Characteristics of Nanocrystalline TWIP Steel Under Uniaxial Tension and Compression, *Mech. Mater.*, 2019, **138**, p 103147
4. J. Park, M. Kang, S.S. Sohn, S.H. Kim, H.S. Kim, N.J. Kim and S. Lee, Quasi-Static and Dynamic Deformation Mechanisms Interpreted by Microstructural Evolution in Twinning Induced Plasticity (TWIP) Steel, *Mater. Sci. Eng. A*, 2017, **684**, p 54–63
5. K.M. Rahman, V.A. Vorontsov and D. Dye, The Effect of Grain Size on the Twin Initiation Stress in a TWIP Steel, *Acta Mater.*, 2015, **89**, p 247–257
6. O. Bouaziz, S. Allain, C.P. Scott, P. Cugy and D. Barbier, High Manganese Austenitic Twinning Induced Plasticity Steels: A Review of the Microstructure Properties Relationships, *Curr. Opin. Solid State Mater. Sci.*, 2011, **15**, p 141–168
7. P. Kusakin, A. Belyakov, C. Haase, R. Kaibyshev and D.A. Molodov, Microstructure Evolution and Strengthening Mechanisms of Fe-23Mn-0.3C-1.5Al TWIP Steel during Cold Rolling, *Mater. Sci. Eng. A*, 2014, **617**, p 52–60
8. O. Bouaziz, C.P. Scott and G. Petitgand, Nanostructured Steel with High work-Hardening by the Exploitation of the Thermal Stability of Mechanically Induced Twins, *Scripta Mater.*, 2009, **60**, p 714–716
9. C. Haase, L.A. Barrales-Mora, F. Roters, D.A. Molodov and G. Gottstein, Applying the Texture Analysis for Optimizing Thermomechanical Treatment of High Manganese Twinning-Induced Plasticity Steel, *Acta Mater.*, 2014, **80**, p 327–340
10. P. Zhou, Z.Y. Liang, R.D. Liu and M.X. Huang, Evolution of Dislocations and Twins in a Strong and Ductile Nanotwinned Steel, *Acta Mater.*, 2016, **111**, p 96–107
11. N.K. Tewary, S.K. Ghosh, S. Bera, D. Chakrabarti and S. Chatterjee, Influence of Cold Rolling on Microstructure, Texture and Mechanical Properties of Low Carbon High Mn TWIP Steel, *Mater. Sci. Eng. A*, 2014, **615**, p 405–415
12. M.M. Abramova, N.A. Enikeev, J.G. Kim, R.Z. Valiev, M.V. Karavaeva and H.S. Kim, Structural and Phase Transformation in a TWIP Steel Subjected to High Pressure Torsion, *Mater. Lett.*, 2016, **166**, p 321–324
13. C. Haase, O. Kremer, W.P. Hu, T. Ingendahl, R. Lapovok and D.A. Molodov, Equal-Channel Angular Pressing and Annealing of a Twinning-Induced Plasticity Steel: Microstructure, Texture, and Mechanical Properties, *Acta Mater.*, 2016, **107**, p 239–253
14. M.S. Matoso, R.B. Figueiredo, M. Kawasaki, D.B. Santos and T.G. Langdon, Processing a Twinning-Induced Plasticity Steel by High-Pressure torsion, *Scripta Mater.*, 2012, **67**, p 649–652
15. J. Ding, Z. Shang, J. Li, H. Wang and X. Zhang, Microstructure and Tensile Behavior of Nanostructured Gradient TWIP Steel, *Mater. Sci. Eng. A*, 2020, **785**, p 139346
16. A. Etemad, G. Dini and S. Schwarz, Accumulative Roll Bonding (ARB)-Processed High-Manganese Twinning Induced Plasticity (TWIP) Steel with Extraordinary Strength and Reasonable Ductility, *Mater. Sci. Eng. A*, 2019, **742**, p 27–32
17. W.X. Yu, B.X. Liu, J.N. He, C.X. Chen, W. Fang and F.X. Yin, Microstructure Characteristics, Strengthening and Toughening Mechanism of Rolled and Aged Multilayer TWIP/Maraging Steels, *Mater. Sci. Eng. A*, 2019, **767**, p 138426
18. A. Azushima, R. Kopp, A. Korhonen, D.Y. Yang, F. Micari, G.D. Lahoti, P. Groche, J. Yanagimoto, N. Tsuji, A. Rosochowski and A. Yanagida, Severe Plastic Deformation (SPD) Processes for Metals, *CIRP Ann.*, 2008, **57**(2), p 716–735
19. A. Azushima and K. Aoki, Properties of Ultrafine-Grained Steel by Repeated Shear Deformation of Side Extrusion Process, *Mater. Sci. Eng. A*, 2002, **337**(1–2), p 45–49
20. A. Yamashita, D. Yamaguchi and Z. Horita, Influence of Processing Temperature on Microstructural Development in Equal Channel Angular Pressing, *Mater. Sci. Eng. A*, 2000, **287**, p 100–106
21. A.R. Eivani and A.K. Taheri, A New Method for Estimating Strain in Equal Channel Angular Extrusion, *J. Mater. Process. Technol.*, 2007, **183**(1), p 148–153
22. I.J. Beyerlein and C.N. Tome, Analytical Modeling of Material Flow in Equal Channel Angular Extrusion, *Mater. Sci. Eng. A*, 2004, **380**(1–2), p 171–190
23. I.B. Timokhina, A. Medvedev and R. Lapovok, Severe Plastic Deformation of a TWIP Steel, *Mater. Sci. Eng. A*, 2014, **593**, p 163–169
24. C. Haase, O. Kremer, W. Hu, T. Ingendahl, R. Lapovok and D.A. Modolov, Equal Channel Angular Pressing and Annealing of a Twinning-Induced Plasticity Steel: Microstructure, Texture and Mechanical Properties, *Acta Mater.*, 2016, **107**, p 239–253
25. E. Bagherpour, M. Reihanian and R. Ebrahimi, On the Capability of Severe Plastic Deformation of Twining Induced Plasticity (TWIP) Steel, *Mater. Des.*, 2012, **36**, p 391–395

26. L. Wang, J.A. Benito, J. Calvo and J.M. Cabrera, Equal Channel Angular Pressing of a TWIP Steel: Microstructure and Mechanical Response, *J. Mater. Sci.*, 2017, **52**, p 6291–6309
27. S. Allain, J.P. Chateau, O. Bouaziz, S. Migot and N. Guelton, Correlations Between the Calculated Stacking Fault Energy and the Plasticity Mechanisms in Fe-Mn-C Alloys, *Mater. Sci. Eng. A*, 2004, **387–389**, p 158–162
28. A. Dumay, J.P. Chateau, S. Allain, S. Migot and O. Bouaziz, Influence of Addition Elements on the Stacking-Fault Energy and Mechanical Properties of an Austenitic Fe-Mn-C Steel, *Mater. Sci. Eng. A*, 2008, **483**, p 184–187
29. S. Vercammen, B. Blanpai, B.C. De Cooman and P. Wollants, Cold Rolling Behaviour of an Austenitic Fe-30Mn-3Al-3Si TWIP-Steel: The Importance of Deformation Twinning, *Acta Mater.*, 2004, **52**, p 2005–2012
30. Y. Iwahashi, Z. Horita, M. Nemoto and T.G. Langdon, An Investigation of Microstructural Evolution During Equal-Channel Angular Pressing, *Acta Mater.*, 1997, **45**, p 4733–4741
31. D. Barbier, N. Gey, S. Allain, N. Bozzolo and M. Humbert, Analysis of the Tensile Behavior of a TWIP Steel Based on the Texture and Microstructure Evolutions, *Mater. Sci. Eng. A*, 2009, **50**, p 196–206
32. L. Chen, H.S. Kim, S.K. Kim and B.C. De Cooman, Localized Deformation due to Portevin–LeChatelier Effect in 18Mn-0.6C TWIP Austenitic Steel, *ISIJ Int.*, 2007, **47**, p 1804–1812
33. L. Li and T.Y. Hsu, Gibbs Free Energy Evaluation of the FCC(γ) and HCP(ε) Phases in Fe-Mn-Si Alloys, *Calphad*, 1997, **21**(3), p 443–448
34. Y.S. Han and S.H. Hong, The effect of Al on Mechanical Properties and Microstructures of Fe-32Mn-12Cr-xAl-0.4C Cryogenic Alloys, *Mater. Sci. Eng. A*, 1997, **222**, p 76–83
35. A. Saeed-Akbari, J. Imlau, U. Prahl and W. Bleck, Derivation and Variation in Composition-Dependent Stacking Fault Energy Maps Based on Subregular Solution Model in High-Manganese Steels, *Metall. Mater. Trans. A*, 2009, **40**(13), p 3076–3090
36. V. Shterner, A. Molotnikov, I. Timokhina and Y. Estrin, A Constitutive Model of the Deformation Behaviour of Twinning Induced Plasticity (TWIP) Steel at Different Temperatures, *Mater. Sci. Eng. A*, 2014, **613**, p 224–231
37. M. Madivala, A. Schwedt, S.L. Wong, F. Roters, U. Prahl and W. Bleck, Temperature Dependent Strain Hardening and Fracture Behavior of TWIP Steel, *Int. J. Plast*, 2018, **104**, p 80–103
38. Y.T. Zhu, X.Z. Liao, X.L. Wu and J. Narayan, Grain Size Effect on Deformation Twinning and Detwinning, *J. Mater. Sci.*, 2013, **13**, p 4467–4475
39. Y.T. Zhu, X.Z. Liao and X.L. Wu, Deformation Twinning in Nanocrystalline Materials, *Prog. Mater. Sci.*, 2012, **57**(1), p 1–62
40. JA Venables, Deformation Twinning in FCC Metals, *Deformation Twinning, Proceedings of a Metallurgical Society Conference. Gainesville, FL, 1963*, Gordon and Breach Science, New York, USA, 1964, p 77–116
41. C.X. Huang, K. Wang, S.D. Wu, Z.F. Zhang, G.Y. Li and S.X. Li, Deformation Twinning in Polycrystalline Copper at Room Temperature and Low Strain Rate, *Acta Mater.*, 2006, **54**, p 655–665
42. C.X. Huang, Y.L. Gao and G. Yang, Bulk Nanocrystalline Stainless Steel Fabricated by Equal Channel Angular Pressing, *J. Mater. Res.*, 2006, **21**(7), p 1687–1692
43. J.E. Jin and Y.K. Lee, Strain Hardening Behavior of a Fe-18Mn-0.6C-1.5Al TWIP Steel, *Mater. Sci. Eng. A*, 2009, **527**, p 157–161
44. J. Yanagimoto, J. Tokutomi, K. Hanazaki and N. Tsuji, Continuous Bending-Drawing Process to Manufacture the Ultrafine Copper Wire with Excellent Electrical and Mechanical Properties, *CIRP Annu. Manuf. Technol.*, 2011, **60**, p 279–282